

## Introduction

Modern satellite radiometers have a large number of detectors. For example, VIIRS has 16 and 32 detectors for the M-band and I-band, respectively, while GOES-R ABI and Advanced Himawari Imager have a few hundred detectors for each band. Since each detector has its own relative spectral response (RSR) and they are not identical, ideally, Sensor Data Record (SDR) or level 1B data should be generated for each detector as if it is an independent detector. However, this is computationally complex and expensive, and the current SDR data is generated based on the band-averaged RSR, treating multiple detectors as one average virtual detector, at the expense of accuracy. We found that the detector level RSR difference does impact VIIRS SDRs in both thermal emissive bands (TEB) and reflective solar bands (RSB). Atmospheric dependencies at detector level top of atmosphere reflectance and brightness temperature differences were observed in the NOAA operational VIIRS SDRs, especially over tropical oceans. Striping is also related to the difference between band-averaged and detector-level RSR. Therefore, if the detector level RSR in SDR processing and calibration is used, the SDR products will more accurately reflect real detector measurements.

The purpose of this study is to investigate the feasibility to use detector level RSR in VIIRS SDR processing and calibration. Here we focus on the TEB bands. New TEB radiance-temperature conversion look-up-tables (LUT) were generated using the detector-level RSR, and the corresponding science code change was studied. The detector-level and band-averaged LUTs were used to generate sample SDR data over the uniform clear-sky ocean surface near tropical and polar regions. Bands M15 and M16 brightness temperatures were analyzed using the sample cases to study the influence of detector-level RSR on TEB striping patterns. In general, the detector-level processing generates more realistic SDR products, but it also may lead to more striping.

## NOAA IDPS Operational SDR Data

The VIIRS radiometric calibration algorithm requires many inputs in the form of input parameters and look-up tables (LUT). The LUTs that are directly used in the per pixel radiometric calibration of Earth view data in TEB include:

1. VIIRS SDR Radiance to Effective Blackbody Temperature (EBBT)
2. VIIRS SDR Emissive (more LUTs are required for TEB calibration)
3. VIIRS SDR HAM Emissive Radiance; 4. VIIRS SDR RTA Emissive Radiance
5. VIIRS SDR OBC Emissive Radiance; 6. VIIRS SDR OBC Reflective Radiance

In the current IDPS SDR products, band-averaged RSRs were used to generate temperature-radiance conversion LUTs [1].

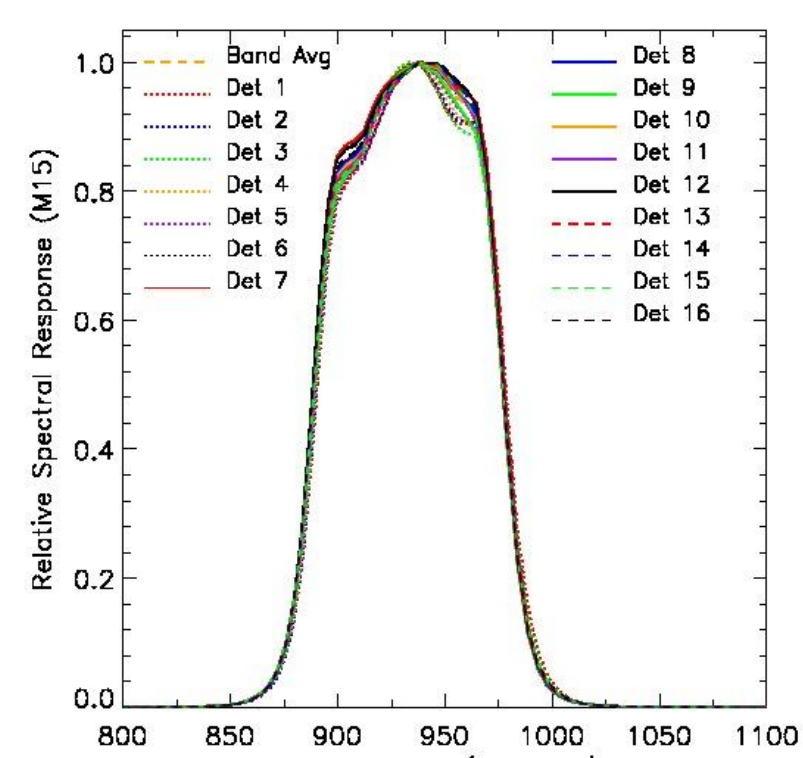


Figure 1. Detector-level and band-averaged relative spectral response (RSR) for M15.

RSR is slightly different among 16 detectors, which will affect the radiance and hence the brightness temperature.

In this study, detector-level temperature-radiance conversion LUTs were generated by considering the difference among detectors. As an example, the detector-level EBBT LUT was generated as following:

- (1) Extract brightness temperature from the band-averaged LUT;
- (2) Compute the blackbody radiance ( $L(\lambda)$ ) from Planck Function using each brightness temperature;
- (3) Convolve  $L(\lambda)$  with detector-level RSR to calculate the in-band averaged radiance, which is corresponding to the brightness temperature for each detector.

## Flowcharts of SDR Processing

Detector-level TEB calibration not only requires detector-level temperature-radiance conversion LUTs, TEB calibration science code also need to be modified to support detector-level processing. Flowcharts of TEB calibration for before and after the code change are shown in Figure 2 and Figure 3

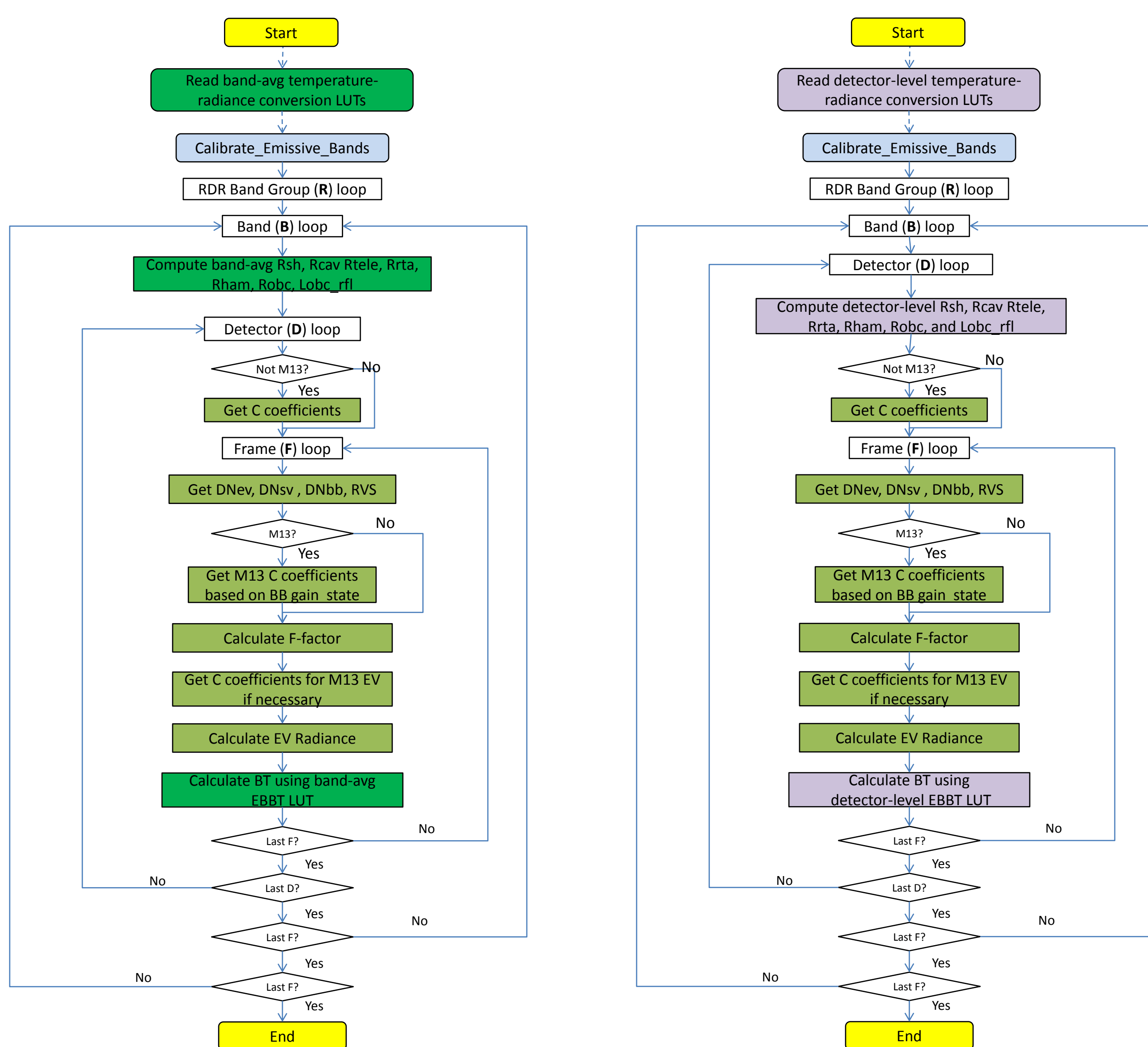


Figure 2. Flowchart of VIIRS TEB processing using band-averaged temperature-radiance conversion LUTs (baseline).

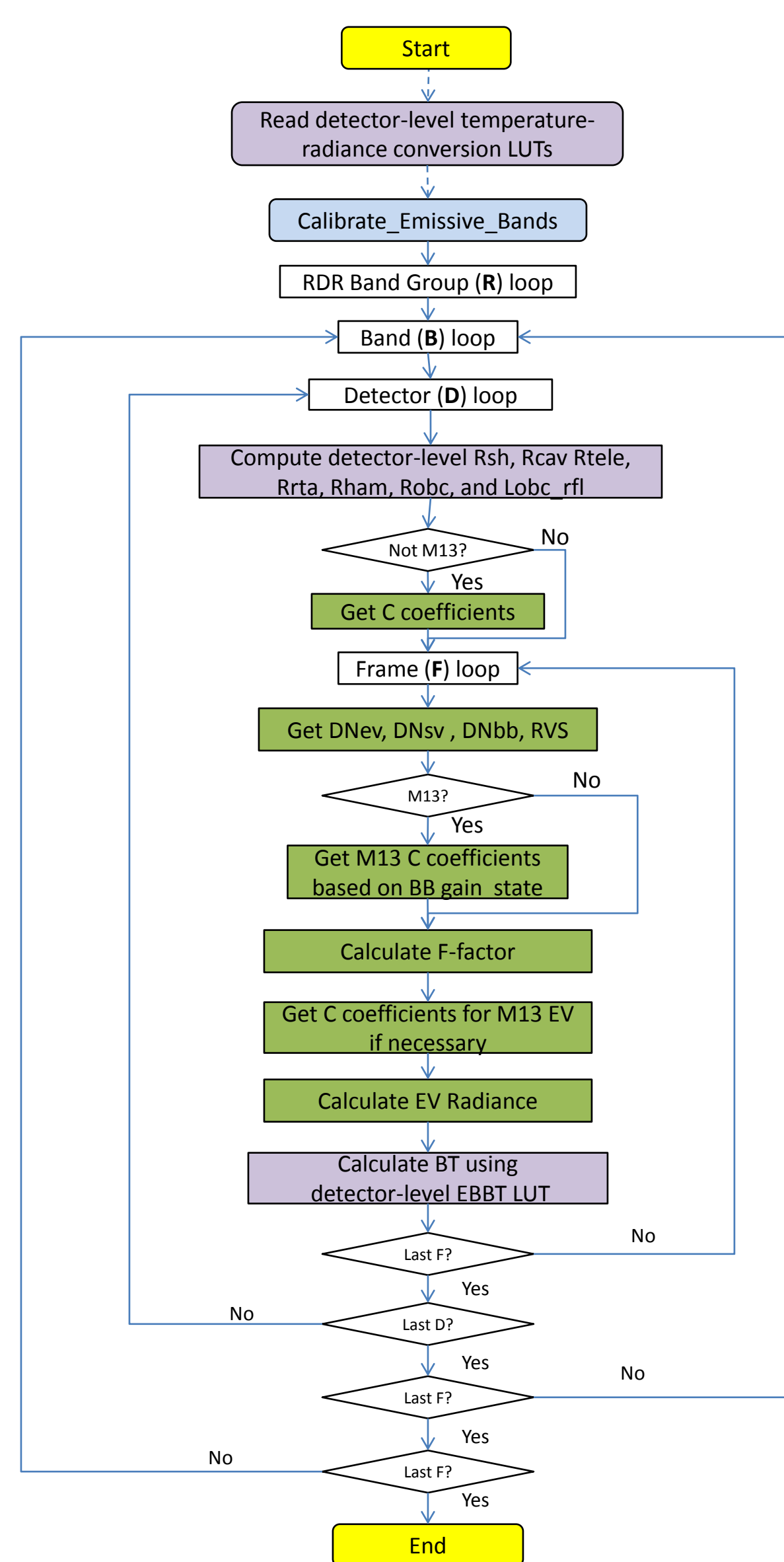


Figure 3. Flowchart of VIIRS TEB processing using detector-level temperature-radiance conversion LUTs (modified).

## Impact of Detector-level RSR on SDRs

In order to investigate the impact of detector-level RSRs on the VIIRS SDR products, M15 and M16 brightness temperatures from sample cases were analyzed. For each case, we selected a small uniform region with size of 60 pixels along scan direction, and 16 scan  $\times$  16 detector along track direction under clear sky condition according to VIIRS Cloud Mask Intermediate Product. Striping patterns were quantified with an index (named VSI). We used the cumulative histogram [2, 3] for striping quantification:

$$H_{i,HAM}(k) = \frac{1}{N_{i,HAM}} \sum_{l=0}^k (\sum_{l \in (l,i,HAM)}) \quad (1)$$

Where the first sum is to count the number of pixels with the value  $l$  (for detector  $i$  and HAM side A or B), and the second sum is over the pixel value  $l$ . In this equation,  $l$  can be BT or BT difference ( $BT_{15}-BT_{16}$ ), which depends on the striping index whether you want to quantify a single band or the band difference. The parameter  $N_{i,HAM}$  is the total number of the pixels in an image for the detector  $i$  and HAM side A or B. Here we didn't separate the HAM side because we focus on the detector level RSR difference instead of HAM side difference in this study.  $H_i$  refers to the percentage of the pixels with value less than  $k$  in an image. If there is striping in an image, the histogram  $H_i$  diverges for different detectors. The divergence of the histogram can be represented as the horizontal distances among the different histograms:

$$g_{i,i'}(P) = k - k' \quad (2)$$

where  $P$  is the percentage of the pixels with the value less than the value in X-axis. X-axis represents the brightness temperatures (BT) or BT difference ( $BT_{15}-BT_{16}$ ). The following relative magnitude, i.e., the ratio of horizontal distance to the X-axis range, is better used to compare among different bands:

$$R = \frac{g(P=50\%)}{\text{Range}_{X-axis}} \quad (3)$$

The larger distance among different histogram corresponds to the stronger striping effects. We have analyzed the difference among 16 detectors (without separating HAM sides) for each small region.

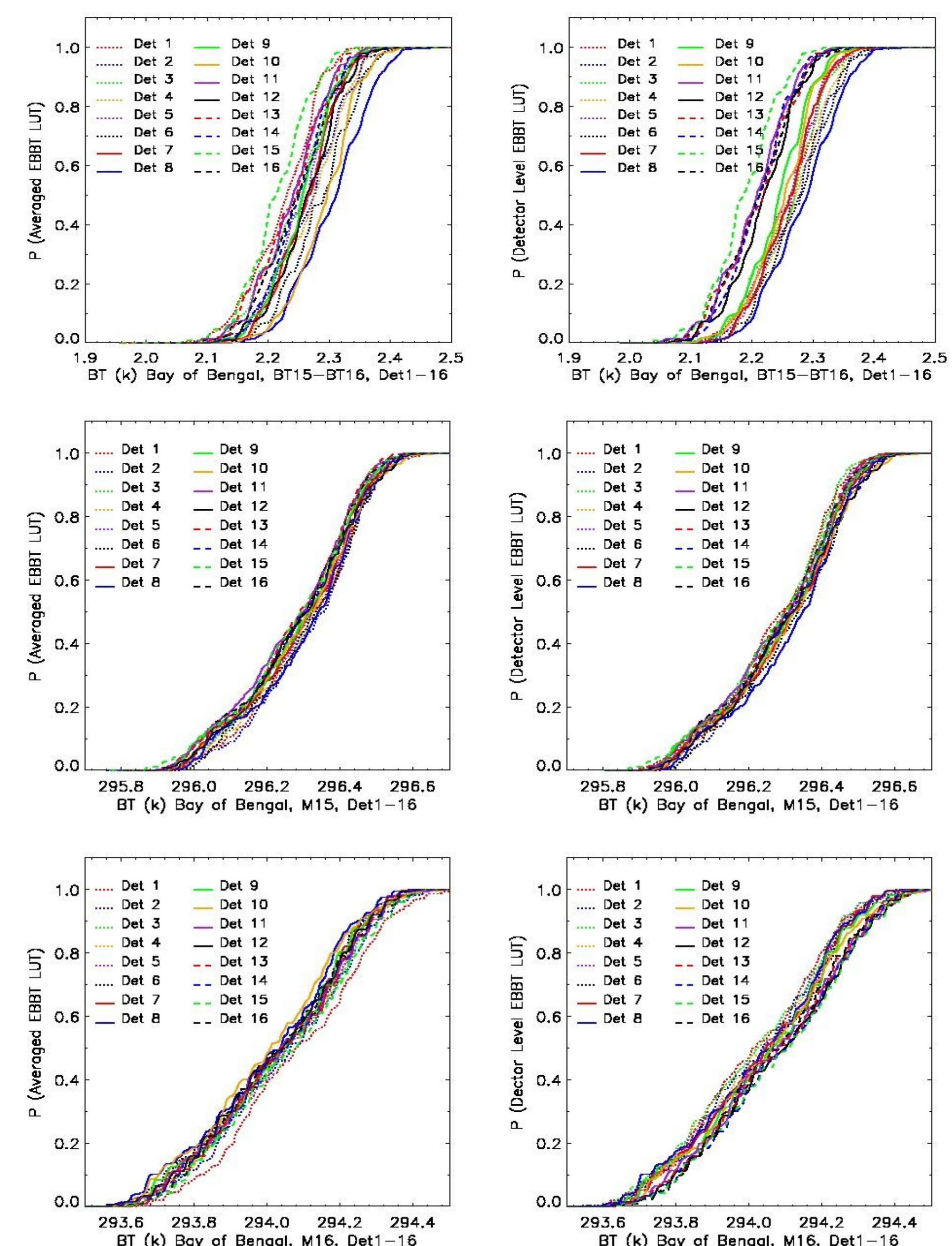


Figure 4. The cumulative histogram for Bay of Bengal over tropical region on 22 June 2014 using the band-averaged RSR (Left) and detector-level RSR (Right) in M15 – M16 (Top), M15 (Middle), and M16 (Bottom).

- Obvious difference between band-averaged and detector-level processing in M15 – M16 (Top) was observed. The histogram is distributed more evenly for the band-averaged processing. For the detector dependent histogram, it separates into three groups: detectors 1,2,3,4,5,6,7,8,9,10; detectors 11,12,13,14,16; and detector 15, which is consistent with the differences in detector-level RSR. The relative magnitude (ratio in Eq.3) in M15 – M16 is increased from 0.099 to 0.105, which means more striping.
- While detector-level processing is closer to reality, it may lead to more horizontal divergence (i.e., more striping) because it reflects the difference among detectors.

## Summary

In this study, we investigated the feasibility of using detector level RSR in VIIRS TEB SDR calibration and processing. The detector-level temperature-radiance conversion LUTs were generated and were used to analyze its impact on the striping in brightness temperature product over the tropical region. The advantage of using detector level RSR is that it can provide more realistic SDR product. However, it also has disadvantage that the RSR difference among detectors also causes the larger horizontal divergence and therefore more striping in SDR brightness temperature product. Further studies are required for the RSB bands in the future.

## References

1. Changyong Cao, and Coauthors (2013): Visible Infrared Imaging Radiometer Suite (VIIRS) Sensor Data Record (SDR) User's Guide, version 1.2.
2. Li, Z.; Yu, F. A Real Time De-Striping Algorithm for Geostationary Operational Environmental Satellite (GOES) 15 Sounder Images. Available online: <http://digitalcommons.usu.edu/cgi/viewcontent.cgi?filename=0&article=1197&context=calcon&type=additonal> (accessed on 6 February 2016).
3. Weinreb, M.P.; Xie, R.R.; Lienesch, J.H.; Crosby, D.S. Destriping GOES images by matching empirical distribution functions. *Remote Sens. Environ.* **1989**, *29*, 185–195.
4. Zhuo Wang and Changyong Cao (2016): Assessing the Effects of Suomi NPP VIIRS M15/M16 Detector Radiometric Stability and Relative Spectral Response Variation on Striping. *Remote Sensing*, *8*(2), 145; doi:10.3990/rs8020145.